

## Using chemistry transport modeling in statistical analysis of stratospheric ozone trends from observations

S. Guillas<sup>1</sup>

Center for Integrating Statistical and Environmental Science, University of Chicago, Chicago, Illinois, USA

M. L. Stein

Department of Statistics, University of Chicago, Chicago, Illinois, USA

D. J. Wuebbles and J. Xia

Department of Atmospheric Sciences, University of Illinois, Urbana, Illinois, USA

Received 20 May 2004; revised 30 July 2004; accepted 9 August 2004; published 17 November 2004.

[1] Since the implementation of the international controls on ozone-depleting chemicals, an important focus in studies of stratospheric ozone has been on the detection of a turnaround in the downward trend. The usual statistical assumption of a piecewise linear representation of the trend does not account for the chemistry involved. Because the actual change is not expected to be piecewise linear, we model the trend using results from a University of Illinois at Urbana-Champaign two-dimensional (UIUC 2-D) chemical transport model of the global atmosphere. As part of the analysis, ozone observations are considered in the spectral domain using a cohesive data set from the SBUV-SBUV/2 satellite system at northern midlatitudes. In this study we find that the new model is better at capturing the long-range correlation of the data than assuming a linear trend. We also compare several statistical trend models, based either on a regression on a linear trend or on the Effective Equivalent Stratospheric Chlorine (EESC). Including a constant halocarbon emissions run of the UIUC 2-D model in the regression, the controlled EESC approach shows the best fit. The smallest future data length necessary to detect a recovery with a certain probability is obtained in this latter case. *INDEX TERMS:* 3210 Mathematical Geophysics: Modeling; 0325 Atmospheric Composition and Structure: Evolution of the atmosphere; 0341 Atmospheric Composition and Structure: Middle atmosphere—constituent transport and chemistry (3334)

**Citation:** Guillas, S., M. L. Stein, D. J. Wuebbles, and J. Xia (2004), Using chemistry transport modeling in statistical analysis of stratospheric ozone trends from observations, *J. Geophys. Res.*, 109, D22303, doi:10.1029/2004JD005049.

### 1. Introduction

[2] The control measures agreed upon internationally in the Montreal Protocol were enforced to trigger a recovery of stratospheric ozone by reducing stratospheric chlorine and bromine. This turning point in ozone is estimated to have begun as early as in the late 1990's according to nine two-dimensional (2-D) models used in the latest international assessment [*World Meteorological Organization (WMO)*, 2003]. The recovery rate depends on chemical, dynamical and radiative processes and the assumed emissions of halocarbons and other gases. In the past, trends have been estimated based on various observational data sources [e.g., *Fioletov et al.*, 2002]. Their statistical inference was addressed by, e.g., *Tiao et al.* [1990], *Weatherhead et al.*

[1998, 2000], and *Reinsel et al.* [2002]. The so-called “hockey stick” model used for deriving a piecewise linear trend with a turnaround, usually chosen in January 1996, is fitted using a linear regression on surrogates for the solar flux, the Quasi Biennial Oscillation (QBO) and the amount of aerosols in the atmosphere.

[3] Instead of fitting a linear trend to the total column ozone time series, we use an analysis of the changes in ozone over the same time period based on outputs from the University of Illinois 2-D (UIUC 2-D) chemical transport model (see, e.g., *Wuebbles et al.* [2001] for a description of the model). *Jackman et al.* [1996] and *Solomon et al.* [1996] also addressed the issue of comparing observed ozone trends and model derived trends, but without statistically checking the model's ability to explain the trend. More recently, nine 2-D models participated in an assessment of past ozone changes, including comparison of the statistically derived trends with observations [*WMO*, 2003, section 4.5.3.4]. Note that *Hadjinicolaou et al.* [2002] and *Chipperfield* [2003] examined the long-term ozone variations using respectively simple and full ozone

<sup>1</sup>Now at School of Mathematics, Georgia Institute of Technology, Atlanta, Georgia, USA.

chemistry 3-D chemistry transport models. They found that the 3-D models are able to adequately reproduce the observed temporal features because they are forced by meteorological analysis constructed from observations. Here we statistically test the ability of the UIUC 2-D model to capture the anthropogenic induced trend. We subtract out from the measurements either the UIUC 2-D calculated trend or an assumed piecewise linear trend, and compute the power spectrum for low frequencies. The study is made on data sets that are deseasonalized and corrected for solar activity, QBO and stratospheric aerosols.

[4] In a second part of the paper, we estimate the relationship between the variation in total column ozone and the levels of chlorine and bromine in the atmosphere. Various studies, including WMO [1995, 1999, 2003], Prather and Watson [1990], and Daniel *et al.* [1995] have used the so-called Equivalent Effective Stratospheric Chlorine (EESC) as a surrogate for the amount of ozone-depleting chemicals. The EESC is computed according to observed and predicted emissions. We break down the ozone trend into a natural variation provided by the UIUC 2-D model run which is driven by the solar and volcanic forcings with constant emissions and an anthropogenic trend associated with the EESC. Accordingly, future emissions scenarios are easier to associate with a response in ozone. Furthermore, we measure an improvement in the overall fit to the data using the information given by the UIUC 2-D model for the natural variation.

## 2. UIUC 2-D Chemical Transport Model

[5] The UIUC two-dimensional chemical radiative transport model is a zonally averaged model of the chemistry and physics of the global atmosphere. The model is often used to study human related and natural forcings on the troposphere and stratosphere, but, because it is zonally averaged, the analysis of tropospheric processes is limited. The model determines the atmospheric distributions of 78 chemically active atmospheric trace constituents. The model domain extends from pole to pole and from the ground to 84 km. A grid element in the model represents 5 degrees of latitude and 1.5 km in log-pressure altitude. In addition to 56 photolytic reactions, the model incorporates 161 thermal reactions in the chemical mechanism, including heterogeneous reactions [see, e.g., Wuebbles *et al.*, 2001; Wei *et al.*, 2001]. Reaction rates and photolysis cross sections in the model are based on recommendations from NASA's Chemical Kinetics Review Panel [e.g., DeMore *et al.*, 1997; Sander *et al.*, 2000].

[6] The transport of chemical species is accomplished through advection, turbulent eddy transport, and convection. Transport of species in the model is self-consistently calculated using the predicted model ozone (and other radiatively important species) and seasonally varying climatological temperatures (based on NCEP analyses). Model transport fields are evaluated by combining the zonal mean momentum equation and the thermodynamic equation into a form that, along with the thermal wind equation, yields a second-order Poisson diagnostic equation for the residual mean meridional stream function. The right hand side of the stream function equation includes the net heating rate term and all wave forcings. The net heating rate is calculated

knowing the temperature and chemical species distributions and includes latent heating. Planetary waves for wave numbers 1 and 2 are included. Stratospheric values of  $K_{yy}$  are calculated using the planetary wave dissipation rate and vorticity for both wave number 1 and 2. Values of  $K_{zz}$  due to gravity waves are evaluated. Larger diffusion coefficients are assigned to the troposphere to mimic fast tropospheric mixing. The model uses a seasonally varying tropospheric  $K_{yy}$ . Convective transport in the model is based on the climatology of Langner *et al.* [1990].

[7] The latest version of the UIUC 2D model, labeled the 2002 version, has some key improvements incorporated in it. All of the upgraded components of this version are briefly described in Table 1. Major upgrades to the solution technique of residual mean meridional circulation (RMMC) and the treatments of atmospheric dynamics were made through better representation of the effects of planetary waves and a more accurate method for determining the RMMC. The treatment of planetary waves with wave numbers 1 and 2 have been updated with better data-based boundary topography and boundary winds. Latent heating and the sensible heat flux are specified based on more physically meaningful analyses. An accurate and fast longwave radiation code for the height of surface to 60 km is adopted in the radiation part of the model. The improvements in the treatment of the infrared radiation and RMMC solution technique are discussed by Choi and Youn [2001]. The zonally averaged temperature and wind fields are specified based on 6 year climatology of the U.K. Met Office (UKMO) reanalysis data. In addition, background diffusion coefficients, which cannot be explicitly obtained in the model, are also tuned for the "leaky pipe" model and the model barrier between tropics, midlatitudes, and polar regions.

[8] In the current version of the model the chemistry has been updated according to the NASA recommendations [Sander *et al.*, 2000]. This particularly affects the nitrogen oxide chemistry, the  $N_2O_5$  and  $ClONO_2$  hydrolysis and several HOCl and HCl reactions. HOBr and HOCl cross sections and the  $O_3$  photolysis quantum yields are updated as well.

[9] All of these changes in the model have resulted in the improved representation of the distributions of age of air (see Figure 1), which means better model transport in the "age of air concept" [Hall and Plumb, 1994; Hall *et al.*, 1999]. The upgraded components make the model mean age distribution closer to the observed features described by Park *et al.* [1999]. Older mean ages in the higher latitudes and altitudes than those by Park *et al.* [1999] are seen and thought to be closer to the observed age of air. For example, around 23–25 km the mean age of the current model in the polar regions is larger than the previous versions, which shows the improved performance of the current model in the vicinity.

[10] While not presented in this paper, the vertical trends show the decrease with altitude (the double peak) found in the observations [e.g., see WMO, 2003, Figure 4–30], and compares extremely well with the upper stratosphere decrease. We did not concentrate on that because, unlike total ozone, we do not have the data to clearly define the global trends in the vertical distribution of ozone across the full range of altitudes of interest.

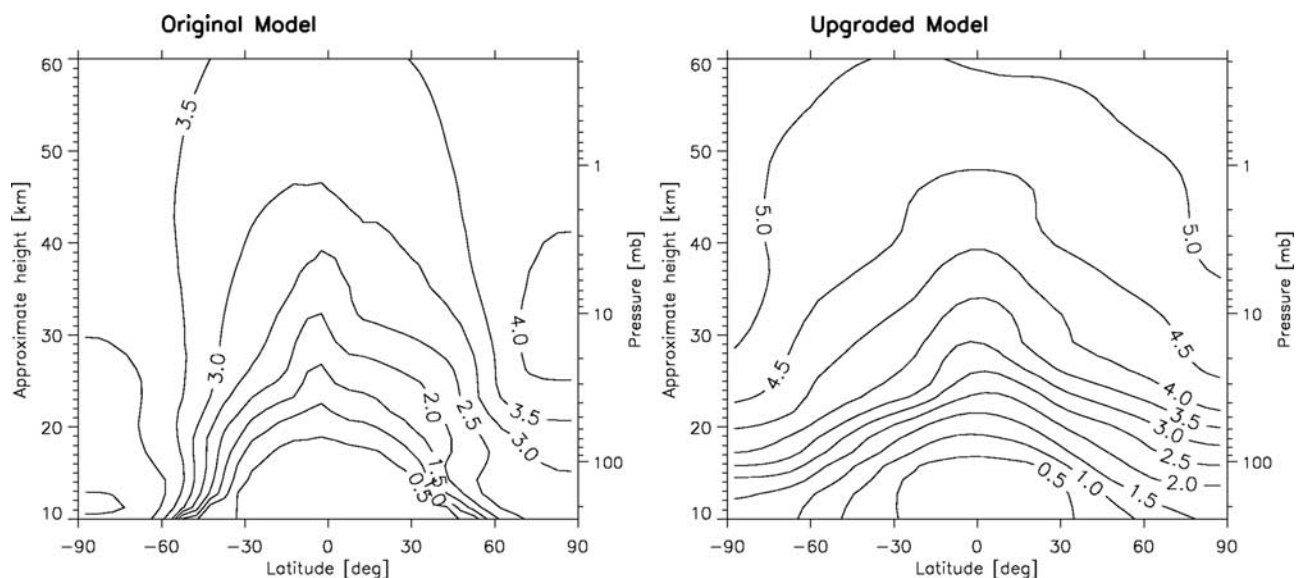
[11] The model describes the response to the solar flux, but does not account for the Arctic Oscillation nor for the

**Table 1.** A Brief Description of the Improved Meteorological Components in the UIUC 2-D Model

Upgraded Model Components	Description	References
RMMC ( $\bar{v}^*$ , $\bar{w}^*$ )	Two schemes of residual mean meridional circulation (RMMC), which target accurate residual circulation in the whole model domain, are applied adequately according to the height levels. It uses both the thermodynamic energy equation and continuity equation among four TEM equations, avoiding tricky and uncertain wave forcings.	<i>Choi [1995], Choi and Youn [2001]</i>
Longwave heating rates $Q_{IR}$	Fast and accurate longwave radiation code for the height range of surface to 60 km is merged to the radiation part of the model. Absorption by CO <sub>2</sub> , O <sub>3</sub> , H <sub>2</sub> O, CH <sub>4</sub> , and N <sub>2</sub> O are atmospheric absorber in the infrared code.	<i>Olaguer et al. [1992], Gettelman et al. [1997]</i>
Latent and sensible heating rates $Q_{latent}$	The results of SNU AGCM (Seoul National University AGCM) are adopted. It is more physical than those from the previous crude parameterization because the algorithm used in the AGCM contains full physical processes in sophisticated manner.	<i>Arakawa and Schubert [1974], Matsuno [1995], Kim [1999]</i>
UKMO meteorological fields	The zonally averaged monthly mean climatologies of wind ( $\bar{U}$ ) and temperature ( $T$ ) field from 6 years of UKMO reanalysis data are used in the model through Fourier time interpolation.	<i>Swinbank and O'Neill [1994], Manney et al. [1996]</i>
Planetary wave model	Rayleigh friction coefficient is found to be very sensitive to amplitudes of wave amplitude in the planetary wave model and so tuned for the better simulation of planetary waves. Planetary wave number 2 was considered as well as wave number 1, with real boundary topographical values and boundary. $K_{yy}$ by planetary wave breaking is parameterized following <i>Garcia [1991]</i> but from full expression of dissipation rates.	<i>Garcia [1991], Garcia et al. [1992], Randel and Garcia [1994], Choi [1996], Li et al. [1995], Nathan et al. [2000]</i>
Background $K_{yy}$	The background values of $K_{yy}$ outside planetary wave breaking region have influence on the global distribution of trace gases. Values of background $K_{yy}$ , $5 \times 10^3 \text{ m}^2 \text{ s}^{-1}$ were chosen for "tropical pipe model" in 2001 model, but these values made tracer distribution away from observed distribution, and so background $K_{yy}$ values are increased and tuned especially in the equatorial region considering height levels such as $0.13 \times 10^6 \text{ m}^2 \text{ s}^{-1}$ from tropopause to 21 km, $0.07 \times 10^6 \text{ m}^2 \text{ s}^{-1}$ from 21 km to 35 km, and $0.1 \times 10^6 \text{ m}^2 \text{ s}^{-1}$ above 35 km for "leaky pipe model." The various different background values of $K_{yy}$ between tropics and midlatitudes are tested and then properly specified. Some changes in the troposphere are also done.	<i>Schoeberl et al. [1997], Shia et al. [1998], Li and Waugh [1999], Schneider et al. [2000], Jones et al. [2001]</i>
$K_{zz}$	Vertical diffusion coefficient $K_{zz}$ values in the troposphere and lower stratosphere were changed. A lower limit of $K_{zz}$ of $0.01\text{--}0.02 \text{ m}^2 \text{ s}^{-1}$ in the lower stratosphere following the observational analysis of <i>Hall and Waugh [1997]</i> and <i>Mote et al. [1998]</i> was specified. However, it makes little difference in the model distribution of trace gases.	<i>Hall et al. [1999], Shia et al. [1998], Bacmeister et al. [1998], Fleming et al. [1999]</i>

QBO. Figure 2 shows the deviations between 30°N and 60°N (area corrected) of total column ozone for the SBUV data set (see section 3). The procedure for the trend retrieval was the so-called Locally Weighted Scatterplot Smoothing (LOESS) technique [see *Cleveland et al., 1990*]. In *WMO [2003, Figure 4.33]* for northern midlatitudes, a seasonal

pattern is removed and four passes of a 13 month running mean were used to smooth the data, and the LOESS procedure is very similar, but we were able to display data from 1980 instead of 1981 with the aforementioned four passes. The model obviously does a good job at replicating the long-term behavior of the satellite data. Figure 2 is only

**Figure 1.** Improved representation of the distributions of age of air for the UIUC 2-D model.

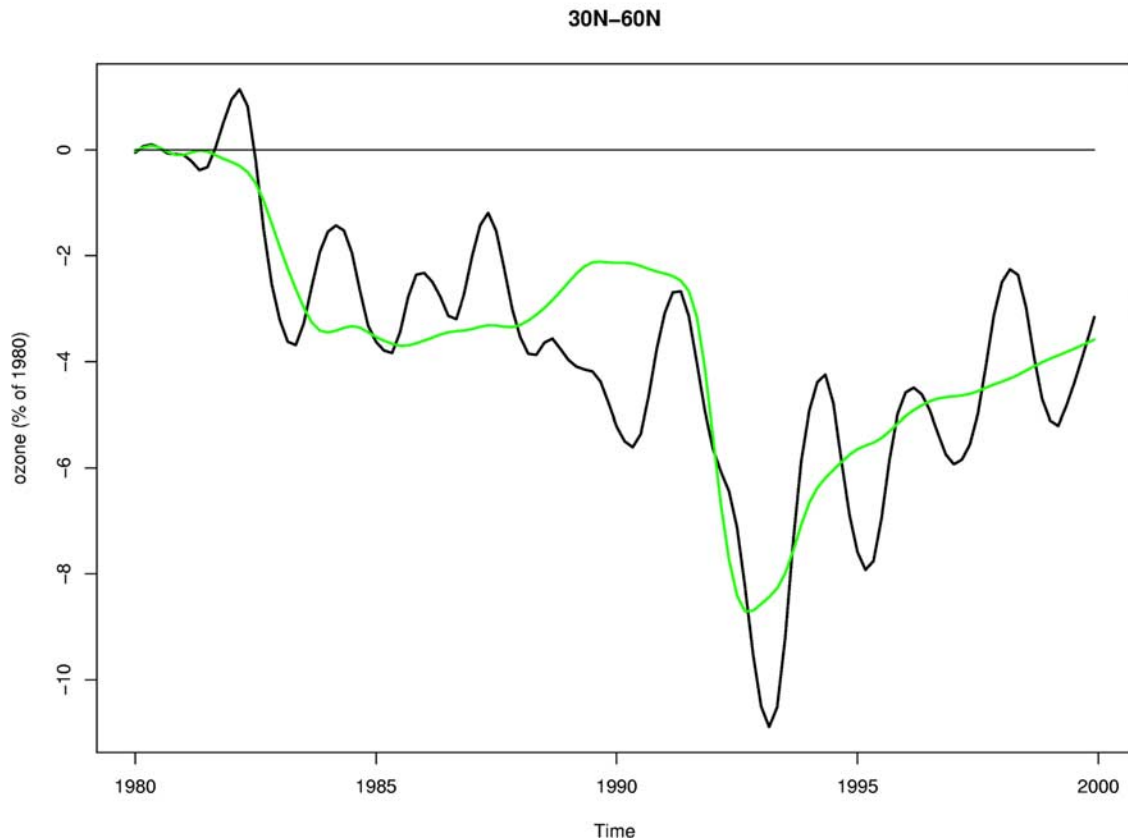


**Figure 2.** Monthly deseasonalized and smoothed measurements SBUV/2 (black) and UIUC 2-D model outputs (green) for  $30^{\circ}$ – $60^{\circ}$ N, January 1980 to December 1999. Changes are calculated in percent with respect to the average 1980 values for each time series.

displayed for illustration purposes. Indeed, in the following sections, we will look at data which were not smoothed in order to examine precisely the month-to-month variability. One should be careful when examining this type of figure because of the amount of smoothing and the strong dependence on the 1980 values which might not be well measured or modeled.

[12] For the studies here to evaluate how well the UIUC 2-D chemical transport model can represent observed trends in stratospheric ozone, we have included as inputs to the model (1) the solar middle and near-ultraviolet radiation (200 to 400 nm) data from 1970 to 2002 (as updated by J. L. Lean (personal communication, 2003), based on earlier analyses by *Lean et al.* [1997]); (2) the surface mixing ratios from [WMO, 2003] for all relevant source gases (e.g., halocarbons, methane, nitrous oxide, carbon monoxide) but updated using recent data from Climate Monitoring and Diagnostics Laboratory (CMDL, using data on <http://www.cmdl.noaa.gov>); (3) stratospheric aerosol surface area densities derived from extinction measurements by Stratospheric Aerosol and Gas Experiment (SAGE) II from 1981 to 2002 (as updated by L. W. Thomason (personal communication, 2003), based on earlier analyses by *Thomason et al.* [1997]); and (4) tropospheric and stratospheric temperature data from 1980 to 2002 based on a combination of analyses for 1000 hPa to 10 hPa based on the National Center for Environmental Prediction/National Center for Atmospheric Research (NCEP/NCAR; <http://dss.ucar.edu/>

pub/reanalysis) reanalysis, and the data from 10 hPa to 0.5 hPa based on NOAA Climate Predict Center (CPC (A. J. Miller, personal communication, 2003)) analyses.

### 3. Data Set

[13] Covering the period ranging from January 1979 to December 2001, the observed data set we use for ozone is a calibrated data set, composed of data sources from multiple satellites. It has been averaged over month, longitude, and binned into  $10^{\circ}$  latitude bands [*Miller et al.*, 2002], forming so-called monthly zonal means. The observations are from the Solar Backscatter Ultraviolet Ozone Sensors (SBUV and SBUV/2). The overlaps between the satellites have been used to estimate their relative biases and adjust all the data sets to the NOAA-9 SBUV/2 as the standard. We examine four latitudinal bands:  $50^{\circ}$ – $60^{\circ}$ N,  $40^{\circ}$ – $50^{\circ}$ N,  $30^{\circ}$ – $40^{\circ}$ N,  $20^{\circ}$ – $30^{\circ}$ N. Three or four months are missing for those bands, and values based on simple linear interpolations were imputed. In comparison to the Total Ozone Mapping Spectrometer (TOMS) zonal averages data set, based on several satellites as well, the SBUV-SBUV/2 data set has no major gaps. There were no TOMS measurements for parts of 1993 and 1994, for the whole year of 1995, and the first half of 1996. *Fioletov et al.* [2002] examined six data sets of monthly average zonal means of total column ozone, including ground-based measurements, and estimated past variations and trends. These analyses clearly demon-

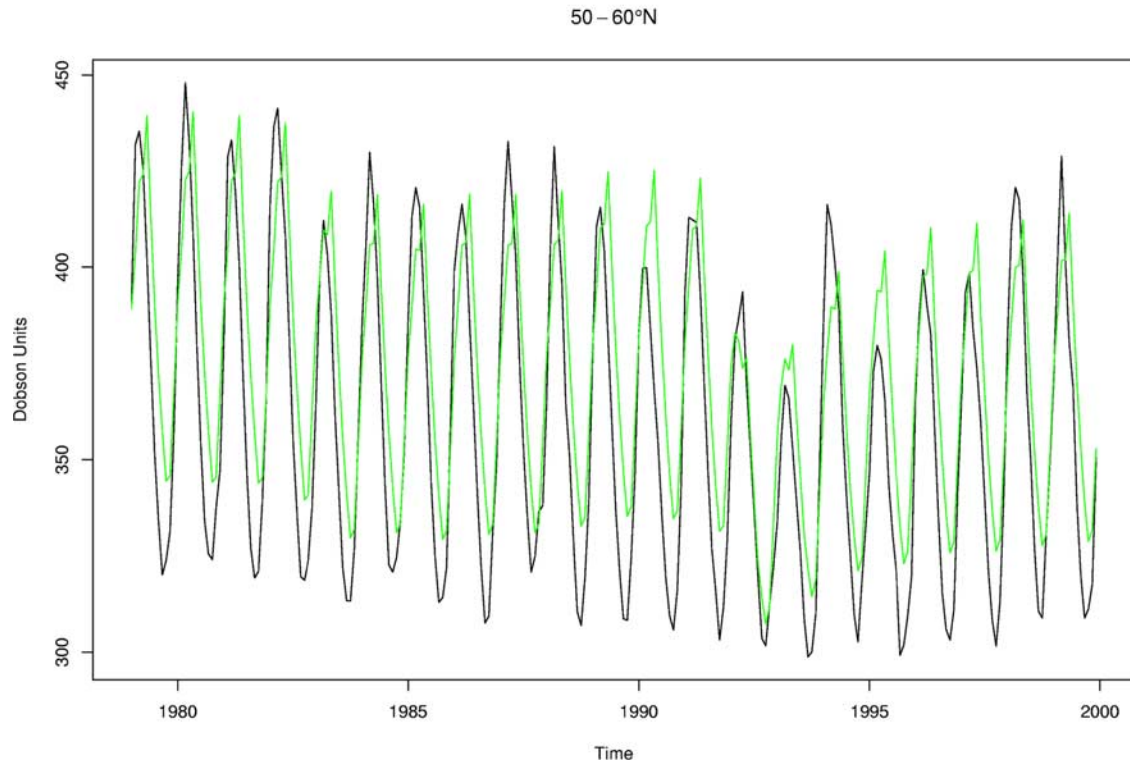


**Figure 3.** Monthly measurements from SBUV/2 (black) and UIUC 2-D model outputs (green) for 50°–60°N, January 1979 to December 1999.

strate problems with ground-based measurements, including that they are inhomogeneous in terms of local ozone “climatology” due to the locations (especially longitude), their calibration, the type of instrument used (e.g., Dobson and Brewer instruments, filter ozonometers), and an unclear systematic bias.

[14] Figure 3 displays a comparison of the monthly SBUV-SBUV/2 measurements and UIUC 2-D outputs. There is a time lag of 15 days between the two data sets. Furthermore, we noticed that the seasonal cycle is not perfectly represented in the model, so a raw shift of 1.5 month lag was performed. The seasonal cycle correction could be improved, and some research is in progress to address this issue. However, our point in this paper is to look for long-term trend assessment, and therefore we used this simple correction.

[15] We carry out a linear regression on monthly indicators, the f10.7 solar flux, the 50 hPa equatorial Quasi Biennial Oscillation (QBO) lagged six months, and a surrogate for volcanic activity: the optical thickness (Northern Hemisphere average, as in <http://www.giss.nasa.gov/data/strataer>). This type of correction has been used in past studies [e.g., *Weatherhead et al.*, 1998, 2000; *Reinsel*, 2002] and optical thickness has been used in trend analyses of Umkehr ozone data [*Reinsel*, 2002]. We regress the UIUC 2-D simulations on the same regressors. We restricted the time period to December 1999, since the optical thickness data were only available until this date. Table 2 shows the regression coefficients of those corrections. Since the QBO was not taken into account by the UIUC 2-D model, the coefficients are logically not significant.

[16] In former statistical trend assessments [e.g., *Weatherhead et al.*, 1998, 2000; *Reinsel*, 2002], a piecewise linear trend was estimated from the data, with an arbitrary (but scientifically meaningful) turnaround occurring in  $T_0 = \text{January 1996}$ . Note that the turnaround is actually very smooth, so that the detection of a recovery is not very sensitive to the starting date. Corrected total column ozone is denoted by  $O(t)$ . Denoting by  $t$  the monthly index, let  $X_{2t} = t/12$  and

$$X_{2t} = \begin{cases} 0 & 0 < t \leq T_0 \\ (t - T_0)/12 & T_0 < t \end{cases}$$

**Table 2.** Summary of Regression Coefficients Estimates<sup>a</sup>

Latitude, °N	Solar	QBO	Aerosol
<i>Measurements</i>			
50–60	6.61 (1.48)	2.54 (0.59)	–84.88 (20.15)
40–50	4.49 (1.29)	3.54 (0.52)	–63.34 (17.61)
30–40	5.62 (0.93)	3.48 (0.37)	–21.68 (12.62)
20–30	5.65 (0.65)	3.15 (0.26)	–17.99 (8.86)
<i>UIUC 2-D Model</i>			
50–60	11.01 (1.10)	0.75 (0.44)	–124.38 (14.94)
40–50	8.56 (0.74)	0.48 (0.30)	–81.35 (10.08)
30–40	6.62 (0.49)	0.29 (0.20)	–50.80 (6.66)
20–30	5.21 (0.33)	0.17 (0.13)	–34.32 (4.55)

<sup>a</sup>Standard errors in parentheses. SBUV/2 measurements and UIUC 2-D model regressed on solar flux (DU per 100 flux), QBO (DU per 10 m/s), and stratospheric aerosol optical thickness at 550 nm. January 1979 to December 1999.

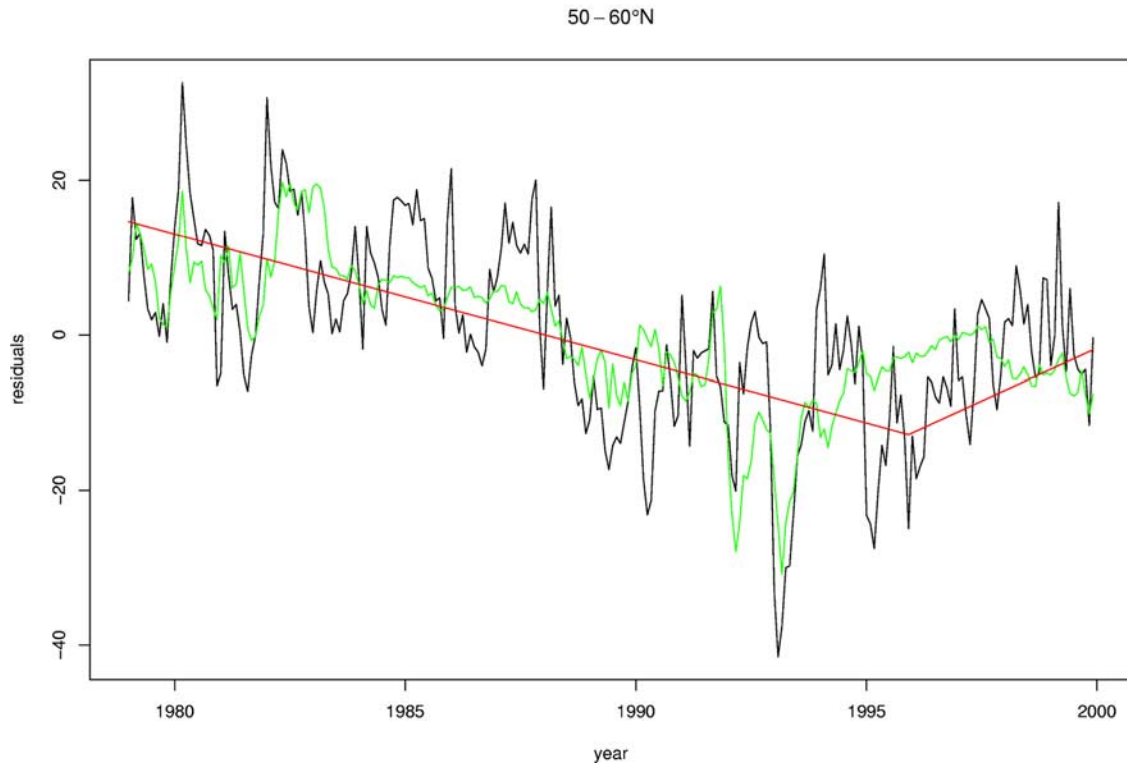


**Figure 4.** Monthly deseasonalized, solar, QBO, and aerosol corrected SBUV/2 data (black), fitted piecewise linear trend (red), and UIUC 2-D model outputs (green) for 50°–60°N, January 1979 to December 1999.

[17] Then the statistical model for the trend is of the form

$$O(t) = c + \omega_1 X_{1t} + a_1 X_{2t} + N_t.$$

$X_{1t}$  is the linear trend before 1996,  $X_{2t}$  is the linear recovery contrasted with  $X_{1t}$ , and  $\omega_1$  and  $a_1$  are the associated rates. The noise  $N_t$  is AR(1), i.e.,  $N_t = \rho N_{t-1} + \epsilon_t$  where  $(\epsilon_t)$  is a sequence of independent identically distributed Normal random variables (white noise) with common variance  $\sigma_\epsilon^2$ . This choice of an AR(1) noise is made because the monthly data measurements show a strong positive autocorrelation due to unexplained large-scale dynamical circulation processes. The AR(1) fit for the residuals has been shown to be satisfactory [e.g., *Tiao et al.*, 1990; *Weatherhead et al.*, 1998, 2000; *Reinsel*, 2002]. *Fioletov and Shepherd* [2003] precisely studied the monthly autocorrelations, showing that they vary by season, and some modeling improvement is to be expected from their findings.

[18] Figure 4 shows for 50°–60°N the monthly corrected data, the fitted piecewise linear trend, and the monthly corrected UIUC 2-D outputs. The atmospheric model clearly follows more closely the natural variation of the data. While the year-to-year fluctuations are smaller, the UIUC 2-D simulations seem to accurately capture the evolution of total column ozone. The observed decrease in ozone after 1997 is likely because of the use of observed temperatures. The optical thickness coefficient used for aerosol correction is mostly significant across latitude, but

the patterns of the residuals after this correction may indicate that the relation between total column ozone and optical thickness is not linear.

#### 4. A Study in the Spectral Domain

[19] To judge how well the model captures the long-term evolution of the total column ozone, we estimate the following power spectra: the power spectrum of the measurements, the power spectrum of the difference measurements minus the UIUC 2-D model trend, and the power spectrum of the difference measurements minus a piecewise linear trend. In Figure 5, one can see how subtracting out the UIUC 2-D model from the data decreases the power magnitude at low frequency more than subtracting out the piecewise linear trend, except for 50°–60°N at very low frequency (about 0.2 cycles/yr or about a 5 year period) where the power is slightly higher for the difference with the UIUC 2-D model. However, as we will see in section 6, the long-term trend assessment either by fitting a piecewise linear trend or by using the UIUC 2-D model is not a direct function of the very low frequency power diminution. Except for 50°–60°N at very low frequency, the UIUC 2-D model does better up to about 0.5 cycles/yr, or about a 2 year period. Furthermore, for 40°–50°N and 50°–60°N, the UIUC 2-D model reduces some relatively high frequency variations (around 1 cycles/yr) more than the linear trend does. In absolute terms, if the power spectrum were flat for the quantity measurements minus UIUC 2-D model, then we

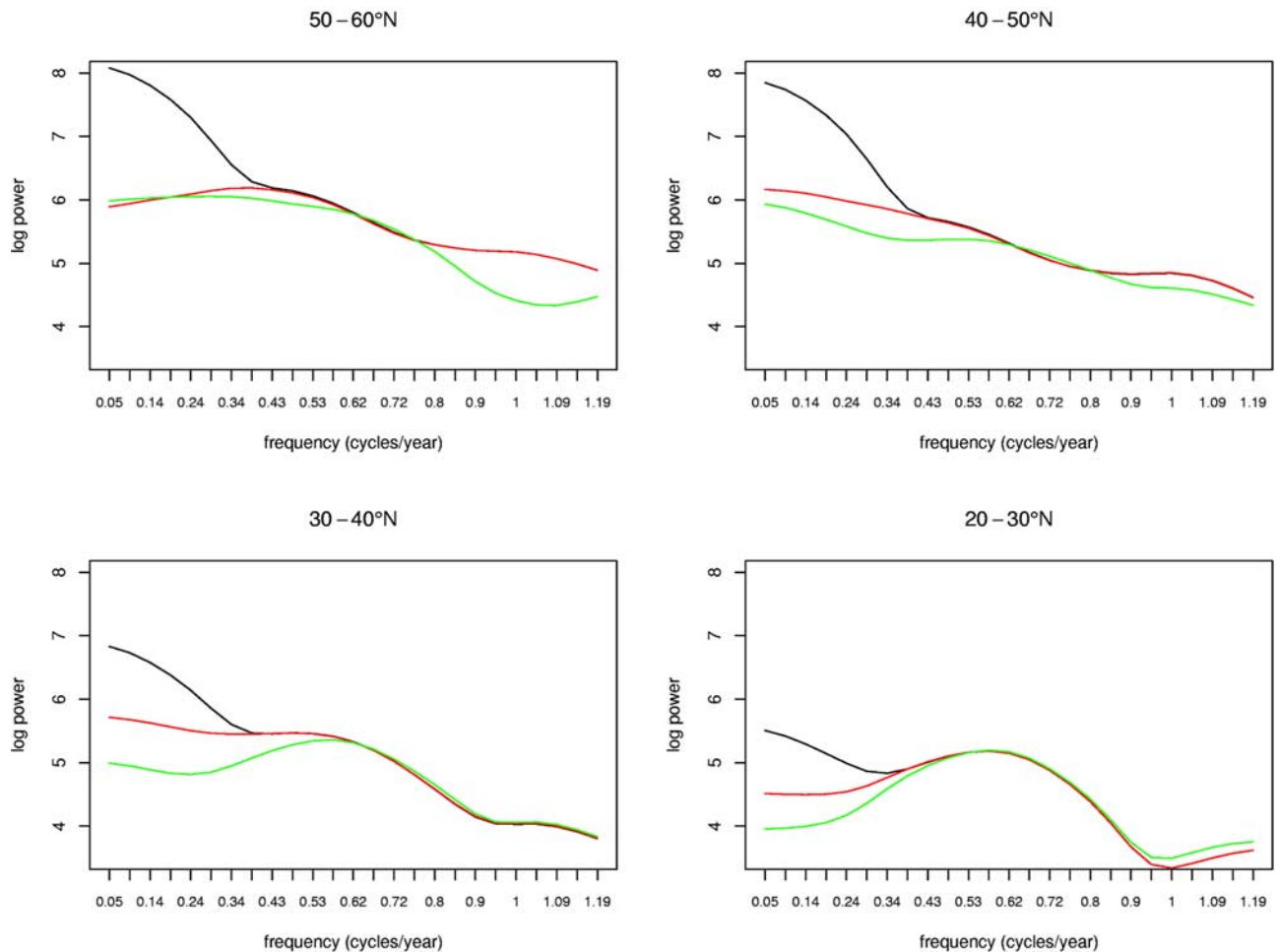


**Figure 5.** Smoothed periodograms for latitudes  $50^{\circ}$ – $60^{\circ}$ N,  $40^{\circ}$ – $50^{\circ}$ N,  $30^{\circ}$ – $30^{\circ}$ N, and  $20^{\circ}$ – $30^{\circ}$ N. Deseasonalized, solar flux, QBO and aerosol corrected SBUV/2 data from January 1979 to December 1999. In black, smoothed periodogram of measurements. Smoothed periodogram of the quantity measurements minus a fitted linear trend (red); smoothed periodogram of the quantity measurements minus UIUC 2-D model based trend (green).

could argue that the model captures the long-term variation of ozone because the power spectrum of a white noise is flat. Note that for an autoregressive process with positive autocorrelation  $\rho$ , the power spectrum is proportional to  $(1 - 2\rho\cos(\omega) + \rho^2)^{-1}$ , where  $\omega$  is the frequency. Hence the power spectrum is decreasing as  $\omega$  increases for low frequencies. For the  $30^{\circ}$ – $40^{\circ}$ N,  $40^{\circ}$ – $50^{\circ}$ N and  $50^{\circ}$ – $60^{\circ}$ N latitude bands, the power spectrum of this difference is not flat. This could be explained by the positive autocorrelation left over in this difference (see section 5), or by the fact that for these latitude bands, the UIUC 2-D model does not completely capture the long-term variation of ozone.

## 5. Chlorine Assessment

[20] The Equivalent Effective Stratospheric Chlorine (EESC) is an index summarizing the amount of ozone-depleting chemicals containing chlorine and bromine. For a thorough description of this concept, see [WMO, 1999,

chap. 11], which we follow here. We calculate the EESC for our scenarios as

$$EESC(t) = \sum_{x \in \text{Cl}} n_x f_x [x]_{t-\text{lag}} + \alpha \sum_{x \in \text{Br}} m_x g_x [x]_{t-\text{lag}},$$

where the first sum is over halocarbons  $x$  containing chlorine and the second sum is over halocarbons containing bromine,  $n_x$  represents the number of chlorine atoms in halocarbon  $x$ ,  $m_x$  represents the number of bromine atoms in halocarbon  $x$ ,  $f_x$  is the relative fractional chlorine release compared to CFC-11,  $g_x$  is the relative fractional bromine release compared to CFC-11, lag is the average estimated transport time required for the halocarbon to travel from the troposphere to the stratosphere, and  $\alpha$  is a measure of the relative impact of bromine compared to chlorine in depleting stratospheric ozone. The estimation of  $\alpha$  is discussed by the WMO [2003, chap. 1] and by Daniel *et al.* [1999]. Figure 6 shows our calculations of the EESC based on either observed emissions and the enforcement of

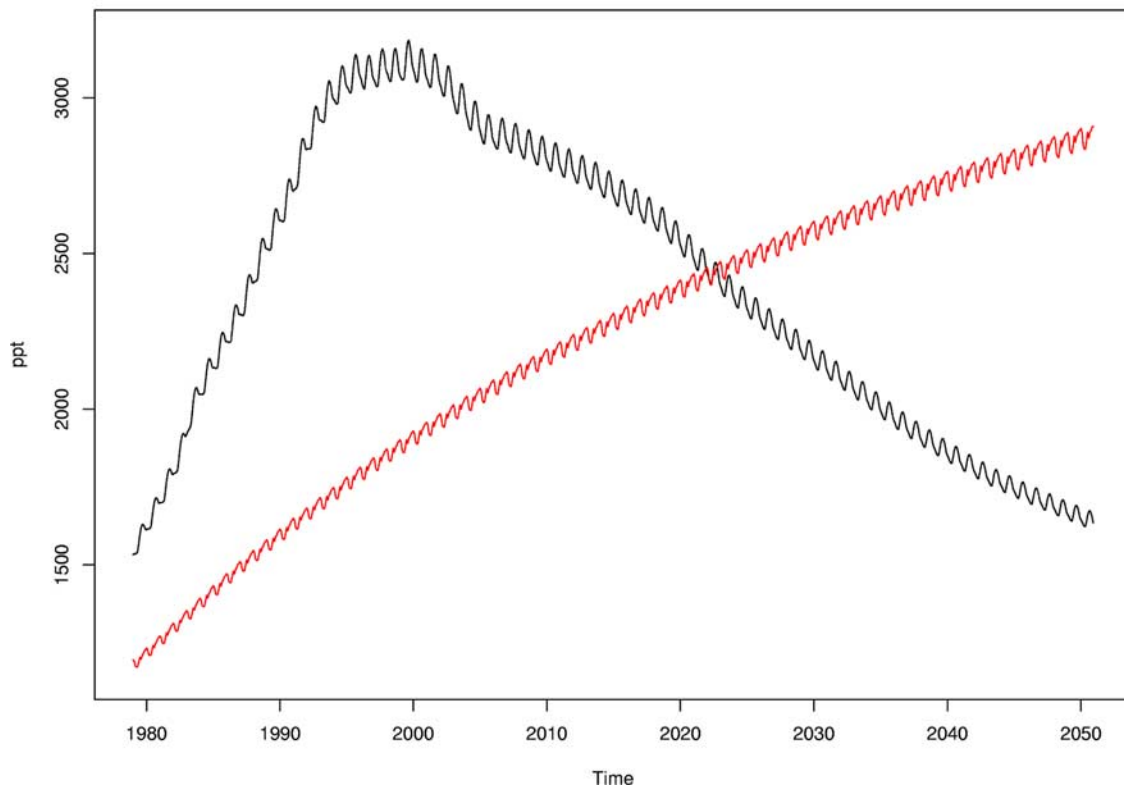


**Figure 6.** Equivalent Effective Stratospheric Chlorine (EESC) in parts per trillion (ppt), January 1979 to December 2050, based on observed emissions and the enforcement of the Montreal protocol and its amendments (black). Equivalent Effective Stratospheric Chlorine (EESC) in parts per trillion (ppt), January 1979 to December 2050, for constant emissions at their 1970 level (red).

the Montreal Protocol and its amendments or the virtual scenario where emissions are kept constant at their level in 1970. We display these time series from January 1979 to December 2050.

[21] *Daniel et al.* [1995] considered that a change in total column ozone can be assumed to be generally proportional to the EESC (our 2-D modeling studies have verified this for the past few decades of ozone changes). However, the ozone loss may turn out to be a nonlinear function of EESC above some threshold [*Daniel et al.*, 1995]. Here, our goal is to better describe the ozone depletion and recovery by dividing the problem into a nonanthropogenic variation of total column ozone and a variation induced by human activity, for which we use the EESC. While there were halocarbon emissions before 1970, the 2-D model assumes that there was no measurable human induced changes in ozone at that time. The nonanthropogenic variation of total column ozone is modeled by a run of the UIUC 2-D model where halocarbon emissions are forced to be equal to their 1970 level during the period ranging from January 1979 to December 1999, and will be denoted by  $G_0(t)$ . Total column ozone is denoted by  $O(t)$ . Both  $O(t)$  and  $G_0(t)$  are solar flux, QBO and aerosol corrected data. We denote by  $C(t)$  and  $C_0(t)$  the respective actual and constant halocarbon emissions scenario EESC loadings across time. We contrast the trend assessment involving the EESC with the piecewise

linear assessment introduced in section 3. We compare the three following regression models. Model 1 is the purely statistical model and fits a piecewise linear trend. Model 2 assumes that the total column ozone change is proportional to the EESC. Model 3 uses total column from the constant emissions run of the 2-D model to explain some of the natural variability in total column ozone not explained by the other factors already in the model. Similar to model 2, it assumes that changes in ozone are proportional to the EESC. Thus we have the following equations:

$$O(t) = c_1 + \omega_1 X_{1t} + a_1 X_{2t} + N_t,$$

$$O(t) = c_2 + a_2 C(t) + N_t,$$

$$O(t) - G_0(t) = c_3 + a_3 (C(t) - C_0(t)) + N_t.$$

In each case,  $N_t$  is assumed to be an AR(1) noise with autocorrelation  $\rho$ :  $N_t = \rho N_{t-1} + \epsilon_t$  where  $\epsilon_t$  is a white noise with variance  $\sigma_\epsilon^2$ .

[22] The justification of the third model resides in the assumption that the UIUC 2-D model is able to simulate the variation in total column ozone not explained by the seasonal cycle, the solar flux, the QBO, the amount of aerosols and the human induced trends better than the statistical model 1 does. For  $50^\circ$ – $60^\circ$  (but it holds as well for the other latitudes), Figure 4 demonstrates that this is a

**Table 3.** Summary of the Trend Estimates for  $\omega_1$  and  $a_1$  in Model 1 (Piecewise Linear Trend With Decay Rate) and Total Contrasted Recovery Rate Given by  $\omega_1$  and  $a_1$ , Respectively) and for the EESC Regression Coefficients  $a$  in Models 2–3<sup>a</sup>

Latitude, °N	$\omega_1$ , DU/yr	$a_1$ , DU/yr	$a_2$ in Model 2, DU/ppb	$a_3$ in Model 3, DU/ppb
50–60	–1.7 (0.3)	6.0 (1.9)	–13.4 (3.2)	–15.9 (4.5)
40–50	–1.4 (0.3)	4.5 (1.7)	–11.6 (2.6)	–14.8 (3.8)
30–40	–0.7 (0.3)	2.0 (1.6)	–6.4 (2.5)	–7.1 (3.6)
20–30	–0.4 (0.2)	1.4 (1.2)	–2.9 (1.9)	–2.2 (3.0)

<sup>a</sup>Standard errors in parentheses. January 1979 to December 1999.

reasonable hypothesis. Therefore model 3 can be labeled a “quasi-controlled experiment”. A controlled experiment removes the effect of confounding variables and focuses on the causal relationship between total column ozone and the EESC. It would be given by the regression  $O(t) - O_0(t) = c_3 + a_3(C(t) - C_0(t)) + N_t$ , where  $O_0(t)$  is the time series of total column ozone under the scenario where the emissions are kept at their 1970 levels. Unfortunately, we are not able to measure this unobservable  $O_0(t)$ . Hence we resort to using  $G_0(t)$  as a surrogate for  $O_0(t)$ . By doing so, we must ensure that we do not introduce a spurious trend due to a possible mismatch between  $O_0(t)$  and  $G_0(t)$ . Indeed, this would bias the estimation of the slope coefficient  $a_3$ , which is our quantity of interest. Thus what we require to avoid bias in our estimate of  $a_3$  is that the mean of  $O_0(t) - G_0(t)$  is constant in time (but not necessarily 0). Figure 5 shows that for the observable  $O(t) - G(t)$ , where  $G(t)$  is the UIUC model simulation under the actual emissions, the periodogram at low frequencies is relatively small, suggesting that at most a relatively small artificial trend is produced by the UIUC model when compared with the observations. Therefore it is reasonable to suppose that this property holds as well for  $O_0(t) - G_0(t)$ . Accordingly, we claim that the coefficient  $a_3$  properly estimates the depletion due to an additional amount of halocarbons containing chlorine or bromine.

[23] Tables 3 and 4 report the results. The Residual Standard Error is an estimate of the noise level  $\sigma_e$ , and therefore gauges the fit. A high autocorrelation implies that a spurious trend induced by the strong dependence in the time series may be confounded with a real trend. The addition from model 2 to model 3 of the constant halocarbon run of the UIUC 2-D model yields an improvement in the fit and the autocorrelation level, especially for high latitudes, as shown in Table 4. For instance, for 40°–50°N, the autocorrelation estimate goes from 0.7624 in model 2 to 0.7108 in model 3. These results support our expectation that the model-based estimate of  $a$  in model 3 is likely to be more accurate than the nonmodel estimate in model 2 where only the EESC index is used, because model 3 better captures the natural variations of ozone that are not linked to the halocarbon emissions. Indeed, some natural variations in model 2 may be attributed to the EESC and the coefficient  $a$  may be inaccurate.

## 6. Detection of a Recovery

[24] Tiao *et al.* [1990] examined the impact of length of data record on trend assessment, especially on the detection

of a recovery. Several studies addressed this issue with greater precision [e.g., Weatherhead *et al.*, 1998, 2000; Reinsel, 2002]. Using a piecewise linear trend, the latter works were able to compute the number of years required to detect a statistically significant recovery. This approach relies on the assumption that the recovery will be linear during the next decades, which may not be true, at least over long time periods, and in times when a turnaround occurs. The key factors in these calculations are the slope, the noise level and the autocorrelation in the data. The question we now address is how many months will it take to determine UIUC 2-D model-derived future trend versus the null hypothesis of no trend. In order to compare with the purely statistical approach where we want to carry out a test for a future linear trend versus no trend, we fit a linear trend to the UIUC 2-D model-derived trends. The difference between these two tests resides in the autoregressive errors associated with the two approaches. As the autocorrelation and Residual Standard Errors (RSE) get smaller, and the slope of the recovery gets steeper, the number of months required to detect a recovery gets smaller too [Weatherhead *et al.*, 2000]. Indeed, if the data are noisy or if the slope is tiny, then it is more difficult to discern an increase. Moreover, with high autocorrelation in the data, e.g., for latitudes closer to the equator (see Table 4), we may confound a recovery with a persistent stochastic variation. Overall, the constant halocarbon run of the UIUC 2-D model with the EESC index (model 3) yields a shorter length of data collection. The last two columns of Table 4 show, for a confidence level of 95%, the number of months necessary to detect a recovery with a probability of either 50% or 90%, starting in January 2000, based on the autocorrelation level, the noise level or Residual Standard

**Table 4.** Summary of the Autocorrelation Estimates and Residual Standard Error (RSE) for Models 1–3<sup>a</sup>

Latitude	Autocorrelation	RSE	Months (50%) <sup>b</sup>	Months (90%) <sup>b</sup>
50°–60°N				
Model 1	0.729 (0.043)	6.303	289	382
Model 2	0.759 (0.041)	6.375	291	400
Model 3	0.724 (0.044)	6.109	154	229
40°–50°N				
Model 1	0.744 (0.042)	5.468	296	394
Model 2	0.762 (0.041)	5.503	292	401
Model 3	0.711 (0.044)	5.381	142	215
30°–40°N				
Model 1	0.819 (0.036)	3.707	393	554
Model 2	0.821 (0.036)	3.713	383	552
Model 3	0.795 (0.038)	3.689	233	326
20°–30°N				
Model 1	0.806 (0.037)	2.961	550	>612
Model 2	0.810 (0.037)	2.967	553	>612
Model 3	0.802 (0.038)	2.952	456	>612

<sup>a</sup>Standard errors in parentheses. Model 1, piecewise linear trend; model 2, EESC-derived trend; model 3, constant-halocarbon run and EESC-derived trends.

<sup>b</sup>Starting in January 2000, necessary to detect a the UIUC 2-D expected recovery at a 95% confidence level with a probability of respectively 50% or 90%, based on the estimated autocorrelation, the RSE computed from January 1979 to December 1999, and the future slope given by the Montreal Protocol’s scenario. Because the chlorine loading simulations only go for 612 months beyond January 2000, when 612 months is not sufficient, we report >612.

Error (RSE), and the future slope obtained from the scenario given by the enforcement of the Montreal Protocol and its amendments. A reasonable estimate of this slope is given by  $a$  in model 2 multiplied by the future EESC. To give more details, first, a detected (positive) slope is deemed statistically significant if the ratio of the estimated slope  $\hat{\omega}$  divided by its estimated standard deviation  $\sigma_{\hat{\omega}}$  is greater than 2, ensuring a 95% confidence level in the detection. The error we would make 5% of the time is detecting a trend when there is no trend, the so-called type I error for this test. Secondly, under the trend predicted by the UIUC 2D model, we require our test to detect it with a specific probability  $1 - \beta$ , called the power of the test. With a power of 50% (i.e.,  $\beta = 0.5$ , half of the actual positive trends are not detected), the detection criterion is still given by  $\hat{\omega} > 2\sigma_{\hat{\omega}}$ . However, if we want to detect 9 out of 10 of the recoveries, that is a power of 90%, the criterion turns out to be  $\hat{\omega} > 3.3\sigma_{\hat{\omega}}$ , yielding longer time periods. For more mathematical details, see Appendix A.

## 7. Conclusion

[25] The statistical analyses indicate that the calculations of past forcings from the UIUC 2-D model succeeds in representing the Northern atmosphere midlatitudes trends of total column ozone when compared to observations from the SBUV/2 satellite-based instrument. Long-term correlations are better estimated than merely fitting a linear trend, as well as shorter-term variability (i.e., 1–3 year period). Moreover, by comparing the model in its version with constant halocarbon emissions to the former statistical method for this region, we lessen the length of the data collection required to detect a recovery. For instance, with a confidence level of 95% and a power for the test of 50% it will take about 142 months instead of 296 months for 40°–50°N. Because of the input of nonhalocarbon emissions (e.g., methane, nitrous oxide), the future recovery in the model does not follow the trend projected by using EESC. Our work suggests that it will be useful to analyze appropriate atmospheric modeling results that adequately integrate the processes affecting future changes in ozone. Previous statistical works had already shown good skills, therefore it could also be interesting to compare enhanced statistical models (e.g., nonlinear regression models, which appear to be more accurate for aerosol correction) with the atmospheric modeling assessment. Another future research area is to study the latitudinal correlation structure [Choi *et al.*, 2002] of the ozone measurements, using the UIUC 2-D model fit. As models for the stratosphere improve, so should the agreement with the observations, and therefore we can expect that the advantages of using our approach versus a purely statistical approach should increase. In particular, 3-D models [e.g., Hadjinicolaou *et al.*, 2002; Chipperfield, 2003] show great promise for this problem since they have a more realistic representation of the dynamical contributions to the ozone trends than 2-D models.

## Appendix A: Statistical Details About the Detection Test

[26] We use the same criteria for trend detection as by Weatherhead *et al.* [1998] and Reinsel [2002], but we apply

our technique to chemical transport model–derived trends. We focus on the following time periods: January 1979 to December 1999 for the estimation of the autocorrelations and the noise level, and January 2000 to December 2050 for the calculation of the number of months required to detect a recovery.

[27] We will reformulate our statistical models from section 5 with the following notations. If  $T$  is the data length in months (starting in January 2000), let  $O$  denote the vector of the future (and therefore unobserved) ozone measurements  $(O(1), \dots, O(T))'$ ,  $C$  the EESC vector under the Montreal Protocol's scenario  $(C(1), \dots, C(T))'$ ,  $C_0 = (C_0(1), \dots, C_0(T))'$  the EESC vector under the scenario with constant emissions since 1970, and  $G_0 = (G_0(1), \dots, G_0(T))'$  the UIUC 2-D vector of ozone levels under the scenario with constant emissions since 1970. To ensure coherent notations, let  $X_1$  be the  $T \times 2$  matrix whose two columns consist of the constant vector  $(1, \dots, 1)'$  and a linear trend indicators  $(1/12, \dots, T/12)'$ ,  $X_2$  the  $T \times 2$  matrix whose columns consist of the constant vector  $(1, \dots, 1)'$  and  $C$ , and  $X_3$  the  $T \times 2$  matrix whose columns consist of the constant vector  $(1, \dots, 1)'$  and  $C - C_0$ . Let  $Y_1 = Y_2 = O$ , and  $Y_3 = O - G_0$  (“adjusted observations” for the third model).

[28] Since the statistical model 1,  $O(t) = c + \omega_1 X_{1t} + a_1 X_{2t} + N_t$ , assumes a recovery starting in 1996 and our starting point is January 2000, only the uncertainty associated with a positive linear trend estimate  $a_1$  that best fits the recovery given by the enforcement of the Montreal Protocol (in model 2) and its amendments will be assessed. Indeed,  $\omega_1$  is then irrelevant. This gives a fair comparison of the methods under the same scenario. Let  $N = (N_1, \dots, N_T)$  be the noise vector. Assume  $N_t$  is an AR(1) noise with autocorrelation  $\rho$ :  $N_t = \rho N_{t-1} + \epsilon_t$  where  $\epsilon_t$  is a white noise with variance  $\sigma_\epsilon^2$ . Our models can be respectively rewritten as the following linear models:

$$Y_1 = X_1 \gamma_1 + N,$$

$$Y_2 = X_2 \gamma_2 + N,$$

$$Y_3 = X_3 \gamma_3 + N,$$

where the  $\gamma$ 's are unknown regression coefficients given by  $\gamma_1 = (c_1, a_1)'$ ,  $\gamma_2 = (c_2, a_2)'$ ,  $\gamma_3 = (c_3, a_3)'$ .

[29] Let  $P'$  be the  $T \times T$  matrix whose diagonal elements are equal to 1, except the  $(1, 1)$  element equal to  $\sqrt{1 - \phi^2}$ , the elements just below the diagonal are equal to  $-\phi$ , and the other elements are 0.  $N$  satisfies  $P'N = \epsilon$ , where  $\epsilon = (\sqrt{1 - \phi^2} N_1, \epsilon_2, \dots, \epsilon_T)'$ . The Generalized Least Squares (GLS) estimates of  $\gamma$  is given in general by  $\hat{\gamma} = (X^{*'} X^*)^{-1} X^{*'} Y^*$ , where  $X^* = P'X$  and  $Y^* = P'Y$ . The covariance matrix of  $\hat{\gamma}$  is

$$\text{Cov}(\hat{\gamma}) = \sigma_\epsilon^2 (X^{*'} X^*)^{-1}.$$

Depending on the model 1, 2 or 3, the  $(2, 2)$  element of  $\text{Cov}(\hat{\gamma})$  is respectively the variance of  $\hat{a}_1, \hat{a}_2, \hat{a}_3$ . Note that a detection of a recovery will test for either  $a_1 > 0$  or  $a_i < 0$  ( $i = 2, 3$ ), since the ozone is depleted by the chlorine and bromine based halocarbons. Under the assumption of a positive specified slope  $a = a_0$ , the (one-sided) test with a 95% confidence (i.e., 5% of the time we classify a

nonrecovery as a recovery) and a power of  $1-\beta$  (i.e., when there is a positive slope, we detect it with a probability of  $1-\beta$ ) is based on the criterion

$$P(\hat{a}_1 > 2\hat{\sigma}_{a_1} | a = a_0) \geq 1 - \beta$$

or

$$P\left(\frac{\hat{a}_1 - a_0}{\hat{\sigma}_{a_1}} > 2 - \frac{a_0}{\hat{\sigma}_{a_1}} | a = a_0\right) \geq 1 - \beta$$

or, using a normal approximation for  $(\hat{a}_1 - a_0)/(\hat{\sigma}_{a_1})$ ,

$$P\left(Z > 2 - \frac{a_0}{\hat{\sigma}_{a_1}}\right) \geq 1 - \beta,$$

with  $Z$  a standard normal random variable. Denoting by  $z_\beta$  the lower  $\beta$  percentile of the standard normal distribution, the last inequality is equivalent to  $2 - \frac{a_0}{\hat{\sigma}_{a_1}} \leq -z_\beta$ . Therefore a detection will be claimed when

$$\hat{\sigma}_{a_1} \leq \frac{a_0}{2 + z_\beta}. \quad (\text{A1})$$

Here,  $a_0$  is given by the future linear trend that best fits the ozone levels under the Montreal Protocol and its amendments.

[30] For models 2 and 3, the technique is exactly the same, except that we use respectively the coefficients  $a_2$  and  $a_3$  associated with the EESC  $C(t)$  or  $C(t) - C_0(t)$ . We then find the smallest number of months such that equation (A1) (or its equivalent for the two latter cases) holds. Table 4 displays these numbers for  $1 - \beta = 0.5$ , which corresponds to  $z_\beta = 0$ , and  $1 - \beta = 0.9$ , which corresponds to  $z_\beta \simeq 1.3$ .

[31] **Acknowledgments.** Although the research described herein has been funded by the U.S. Environmental Protection Agency through STAR Cooperative Agreement R-82940201-0 to the University of Chicago, it has not been subjected to the agency's required peer and policy review and therefore does not necessarily reflect the views of the agency, and no official endorsement should be inferred. The atmospheric modeling studies were supported in part by EPA's Global Programs Division and by the NASA ACPMAP program. A special thank you to Ken Patten for maintaining the atmospheric model. The QBO data comes from the Berlin Stratospheric Data (<http://strat-www.met.fu-berlin.de/products/cdrom/data/qbo>), and the stratospheric optical thickness data set was supplied by the Goddard Institute for Space Studies (<http://www.giss.nasa.gov/data/strataer>). We are grateful to the Editor and two reviewers for comments that improved the quality of the paper. Finally, we wish to thank our late colleague, Gregory C. Reinsel, for his valuable comments.

## References

- Arakawa, A., and W. H. Schubert (1974), Interactions of cumulus cloud ensemble with the large-scale environment. Part I, *J. Atmos. Sci.*, *31*, 671–701.
- Bacmeister, J. T., D. E. Siskind, M. E. Summers, and S. D. Eckermann (1998), Age of air in a zonally averaged two-dimensional model, *J. Geophys. Res.*, *101*, 1457–1461.
- Chipperfield, M. P. (2003), A three-dimensional model study of long-term mid-high latitude lower stratosphere ozone changes, *Atmos. Chem. Phys.*, *3*, 1253–1265.
- Choi, W. (1995), On the meridional circulation in the transformed Eulerian mean system, *J. Korean Meteorol. Soc.*, *31*, 325–337.
- Choi, W. (1996), Eddy mixing by the planetary wave in the stratosphere, *J. Korean Meteorol. Soc.*, *32*, 41–50.
- Choi, W., and D. Youn (2001), Effects of physical and numerical schemes on model-calculated ozone distribution in the stratosphere, *K. J. Atmos. Sci.*, *3*, 39–52.
- Choi, D., G. C. Tiao, and M. L. Stein (2002), A statistical model for latitudinal correlations of satellite data, *J. Geophys. Res.*, *107*(D16), 4295, doi:10.1029/2000JD000246.
- Cleveland, R. B., W. S. Cleveland, J. E. McRae, and I. Terpenning (1990), STL: A seasonal-trend decomposition procedure based on loess, *J. Off. Stat.*, *6*, 3–73.
- Daniel, J. S., S. Solomon, and D. L. Albritton (1995), On the evaluation of halocarbon radiative forcing and global warming potentials, *J. Geophys. Res.*, *100*, 1271–1286.
- Daniel, J. S., S. Solomon, R. W. Portmann, and R. R. Garcia (1999), Stratospheric ozone destruction: The importance of bromine relative to chlorine, *J. Geophys. Res.*, *104*, 23,871–23,880.
- DeMore, W. B., S. P. Sander, D. M. Golden, R. F. Hampson, M. J. Kurylo, C. J. Howard, A. R. Ravishankara, C. E. Kolb, and M. J. Molina (1997), Chemical kinetics and photochemical data for use in stratospheric modeling, *Eval. 12, Publ. 97-4*, Jet Propul. Lab., Pasadena, Calif.
- Fioletov, V. E., and T. G. Shepherd (2003), Seasonal persistence of mid-latitude total ozone anomalies, *Geophys. Res. Lett.*, *30*(7), 1417, doi:10.1029/2002GL016739.
- Fioletov, V. E., G. E. Bodeker, A. J. Miller, R. D. McPeters, and R. Stolarski (2002), Global and zonal total ozone variations estimated from ground-based and satellite measurements: 1964–2000, *J. Geophys. Res.*, *107*(D22), 4647, doi:10.1029/2001JD001350.
- Fleming, E. L., C. H. Jackman, R. S. Stolarski, and D. B. Considine (1999), Simulation of stratospheric tracers using a improved empirically based two-dimensional model transport formulation, *J. Geophys. Res.*, *104*, 23,911–23,934.
- Garcia, R. R. (1991), Parameterization of planetary wave breaking in the middle atmosphere, *J. Atmos. Sci.*, *48*, 1405–1419.
- Garcia, R. R., F. Stordal, S. Solomon, and J. T. Kiehl (1992), A new numerical model of the middle atmosphere: 1. Dynamics and transport of tropospheric source gases, *J. Geophys. Res.*, *97*, 12,967–12,991.
- Gettelman, A., J. R. Holton, and K. H. Rosenlof (1997), Mass fluxes of O<sub>3</sub>, CH<sub>4</sub>, N<sub>2</sub>O and CF<sub>2</sub>Cl<sub>2</sub> in the lower stratosphere calculated from observational data, *J. Geophys. Res.*, *102*, 19,149–19,159.
- Hadjinicolaou, P., A. Jrrar, J. A. Pyle, and L. Bishop (2002), The dynamically driven long-term trend in stratospheric ozone over northern mid-latitude, *Q. J. R. Meteorol. Soc.*, *128*, 1393–1412.
- Hall, T. M., and R. A. Plumb (1994), Age as a diagnostic of stratospheric transport, *J. Geophys. Res.*, *99*, 1059–1069.
- Hall, T. M., and D. Waugh (1997), Tracer transport in the tropical stratosphere due to vertical diffusion and horizontal mixing, *Geophys. Res. Lett.*, *24*, 1383–1386.
- Hall, T. M., D. W. Waugh, K. A. Boering, and R. A. Plumb (1999), Evaluation of transport in stratospheric models, *J. Geophys. Res.*, *104*, 18,815–18,839.
- Jackman, C. H., E. L. Fleming, S. Chandra, D. B. Considine, and J. E. Rosenfield (1996), Past, present, and future modeled ozone trends with comparisons to observed trends, *J. Geophys. Res.*, *101*, 28,753–28,767.
- Jones, D. B. A., A. E. Andrews, H. R. Schneider, and M. B. McElroy (2001), Constraints on meridional transport in the stratosphere imposed by the mean age of air in the lower stratosphere, *J. Geophys. Res.*, *106*, 10,243–10,256.
- Kim, J. K. (1999), Parameterization of land surface processes in an atmospheric general circulation model, Ph.D. thesis, 178 pp., Seoul Natl. Univ., Korea.
- Langner, J., H. Rodhe, and M. Olofsson (1990), Parameterization of sub-grid scale vertical tracer transport in a global two-dimensional model of the troposphere, *J. Geophys. Res.*, *95*, 13,691–13,706.
- Lean, J. L., G. J. Rottman, H. L. Kyle, T. N. Woods, J. R. Hickey, and L. C. Puga (1997), Detection and parameterization of variations in solar mid- and near-ultraviolet radiation (200–400 nm), *J. Geophys. Res.*, *102*, 29,939–29,956.
- Li, S., and D. W. Waugh (1999), Sensitivity of mean age and long-lived tracers to transport parameters in a two-dimensional model, *J. Geophys. Res.*, *104*, 30,559–30,569.
- Li, L., T. R. Nathan, and D. J. Wuebbles (1995), Topographically forced planetary wave breaking in the stratosphere, *Geophys. Res. Lett.*, *22*, 2953–2956.
- Manney, G. L., R. Swinbank, S. T. Massie, M. E. Gelman, A. J. Miller, R. Nagatani, A. O'Neill, and R. W. Zurek (1996), Comparison of U.K. Meteorological Office and U.S. National Meteorological Center stratospheric analysis during northern and southern winter, *J. Geophys. Res.*, *101*, 10,311–10,334.
- Matsuno, T. (1995), Climate system dynamics and modeling, report, 341 pp., Cent. for Clim. Syst. Res. Univ. of Tokyo, Japan.
- Miller, A. J., et al. (2002), A cohesive total ozone data set from the SBUV(2) satellite system, *J. Geophys. Res.*, *107*(D23), 4701, doi:10.1029/2001JD000853.

- Mote, P. W., T. J. Dunkerton, M. E. McIntyre, E. A. Ray, P. H. Haynes, and J. M. Russell (1998), Vertical velocity, vertical diffusion, and dilution by midlatitude air in the tropical lower stratosphere, *J. Geophys. Res.*, *103*, 8651–8666.
- Nathan, T. R., E. C. Cordero, L. Li, and D. J. Wuebbles (2000), Effects of planetary wave-breaking on the seasonal variation of total column ozone, *Geophys. Res. Lett.*, *27*, 1907–1910.
- Olaguier, E. P., H. Yang, and K. K. Tung (1992), A reexamination of the radiative balance of the stratosphere, *J. Atmos. Sci.*, *49*, 1242–1263.
- Park, J. H., M. K. W. Ko, C. H. Jackman, R. A. Plumb, and K. H. Sage (Eds.) (1999), *Models and Measurements II*, 496 pp., NASA Langley Res. Cent., Hampton, Va.
- Prather, M. J., and R. T. Watson (1990), Stratospheric ozone depletion and future levels of atmospheric chlorine and bromine, *Nature*, *344*, 729–734.
- Randel, W., and R. Garcia (1994), Application of a planetary wave breaking parameterization to stratospheric circulation statistics, *J. Atmos. Sci.*, *51*, 1157–1168.
- Reinsel, G. C. (2002), Trend analysis of upper stratospheric Umkehr ozone data for evidence of turnaround, *Geophys. Res. Lett.*, *29*(10), 1451, doi:10.1029/2002GL014716.
- Reinsel, G. C., E. C. Weatherhead, G. C. Tiao, A. J. Miller, R. M. Nagatani, D. J. Wuebbles, and L. E. Flynn (2002), On detection of turnaround and recovery in trend for ozone, *J. Geophys. Res.*, *107*(D10), 4078, doi:10.1029/2001JD000500.
- Sander, S. P., R. R. Friedl, W. B. DeMore, D. M. Golden, M. J. Kurylo, R. F. Hampson, R. E. Huie, G. K. Moortgat, A. R. Ravishankara, C. E. Kolb, and M. J. Molina (2000), Chemical kinetics and photochemical data for use in stratospheric modeling, supplement to Evaluation 12: Update of key reactions, *Publ. 00-3*, Jet Propul. Lab., Pasadena, Calif.
- Schneider, H. R., D. B. A. Jones, and M. B. McElroy (2000), Analysis of residual mean transport in the stratosphere: I. Model description and comparison with satellite data, *J. Geophys. Res.*, *105*, 19,991–20,011.
- Schoeberl, M. R., A. E. Roche, J. M. Russell III, D. Ortland, P. B. Hays, and J. W. Waters (1997), An estimation of the dynamical isolation of the tropical lower stratosphere using UARS wind and trace gas observations of the quasi-biennial oscillation, *Geophys. Res. Lett.*, *24*, 53–56.
- Shia, R.-L., M. K. W. Ko, D. K. Weisenstein, C. Scott, and J. Rodriguez (1998), Transport between the tropical and midlatitude lower stratosphere: Implications for ozone response to high-speed civil transport emissions, *J. Geophys. Res.*, *103*, 25,435–25,446.
- Solomon, S., R. W. Portmann, R. R. Garcia, L. W. Thomason, L. R. Poole, and M. P. McCormick (1996), The role of aerosol variations in anthropogenic ozone depletion at northern midlatitudes, *J. Geophys. Res.*, *101*, 6713–6728.
- Swinbank, R., and A. O'Neill (1994), Quasi-biennial and semi-annual oscillations in equatorial wind fields constructed by data assimilation, *Geophys. Res. Lett.*, *21*, 2099–2102.
- Thomason, L. W., L. R. Poole, and T. R. Deshler (1997), A global climatology of stratospheric aerosol surface area density as deduced from SAGE II: 1984–1994, *J. Geophys. Res.*, *102*, 8967–8976.
- Tiao, G. C., G. C. Reinsel, D. M. Xu, J. H. Pedrick, X. D. Zhu, A. J. Miller, J. J. Deluisi, C. L. Mateer, and D. J. Wuebbles (1990), Effects of autocorrelation and temporal sampling schemes on estimates of trend and spatial correlation, *J. Geophys. Res.*, *95*, 20,507–20,517.
- Weatherhead, E. C., et al. (1998), Factors affecting the detection of trends: Statistical considerations and applications to environmental data, *J. Geophys. Res.*, *103*, 17,149–17,161.
- Weatherhead, E. C., et al. (2000), Detecting the recovery of total column ozone, *J. Geophys. Res.*, *105*, 22,201–22,210.
- Wei, C.-F., S. M. Larson, K. O. Patten, and D. J. Wuebbles (2001), Modeling of ozone reactions on aircraft-related soot in the upper troposphere and lower stratosphere, *Atmos. Environ.*, *35*, 6167–6180.
- World Meteorological Organization (WMO) (1995), *Scientific Assessment of Ozone Depletion: 1994, Rep. 37*, Global Ozone Res. and Monit. Proj., Geneva, Switzerland.
- World Meteorological Organization (WMO) (1999), *Scientific Assessment of Ozone Depletion: 1998, Rep. 44*, Global Ozone Res. and Monit. Proj., Geneva, Switzerland.
- World Meteorological Organization (WMO) (2003), *Scientific Assessment of Ozone Depletion: 2002, Rep. 47*, Global Ozone Res. and Monit. Proj., Geneva, Switzerland.
- Wuebbles, D. J., K. O. Patten, M. T. Johnson, and R. Kotamarthi (2001), New methodology for Ozone Depletion Potentials of short-lived compounds: n-Propyl bromide as an example, *J. Geophys. Res.*, *106*, 14,551–14,571.

---

S. Guillas, School of Mathematics, Georgia Institute of Technology, 686 Cherry Street, Atlanta, GA 30332-0160, USA. (guillas@math.gatech.edu)

M. L. Stein, Department of Statistics, University of Chicago, 5734 S. University Avenue, Chicago, IL 60637, USA. (stein@galton.uchicago.edu)

D. J. Wuebbles and J. Xia, Department of Atmospheric Sciences, University of Illinois, Urbana-Champaign, Atmospheric Sciences Building, 105 S. Gregory Street, Urbana, IL 61801, USA. (wuebbles@atmos.uiuc.edu; jxia@atmos.uiuc.edu)